UDK 669.15-194.57:620.178.2:536.483
Original scientific article/Izvirni znanstveni članek

ISSN 1580-2949
MTAEC9, 57(2)191(2023)

ENHANCING THE CRYOGENIC IMPACT TOUGHNESS OF FERRITIC STEEL BY MULTI-TYPE AND FINE-MICROSTRUCTURE DESIGN

IZBOLJŠANJE KRIOGENSKE UDARNE ŽILAVOSTI FERITNEGA JEKLA Z OBLIKOVANJEM MEŠANE DROBNO ZRNATE MIKROSTRUKTURE

Zi-cheng Liu[1], Peng Gao[*,2], Jia-kuan Ren[3], Cheng-gang Li[3], Wu-bo Zhong[1], Zhan Hu[1], Zhen-yu Liu[*,3]

[1]Zhanjiang iron and Steel Co., Ltd., Baosteel, Zhanjiang 524000, People's Republic of China
[2]Jiujiang University, School of Mechanical and Intelligent Manufacturing, Jiujiang 332005, People's Republic of China
[3]Northeastern University, State Key Laboratory of Rolling and Automation, Shenyang 110819, People's Republic of China

Prejem rokopisa – received: 2020-12-14; sprejem za objavo – accepted for publication: 2023-02-24

doi:10.17222/mit.2020.234

Based on pure melting, multi-type and fine-microstructure design, a ferritic steel with an outstanding combination of cryogenic impact toughness and strength was fabricated. The microstructure was characterized by means of optical microscopy, electron back-scattered diffraction and transmission electron microscopy. The steels with different final cooling temperatures of 663 °C and 560 °C show ferrite and perlite microstructure, and ferrite grain size can be refined from 3.15 μm to 2.67 μm by lowering the final cooling temperature from 663 °C to 560 °C. Moreover, a higher volume fraction of acicular ferrite and polygonal ferrite can be obtained for a lower final cooling temperature of 560 °C. Hence, the cryogenic impact toughness can be enhanced, and the brittle failure can be suppressed, even at –110 °C, showing a higher impact toughness compared with other ferritic steels.

Keywords: Ferritic steel; thermo-mechanical control process; ferrite grain morphology, cryogenic impact toughness

Avtorji so s pomočjo čistega taljenja oziroma uporabe zelo čistih osnovnih surovin in oblikovanja mešane drobno zrnate mikrostrukture izdelali feritno jeklo z izjemno kombinacijo kriogene udarne žilavosti oz. udarne žilavosti pri zelo nizkih temperaturah in mehanske trdnosti. Mikrostrukturo izdelanega jekla so okarakterizirali s pomočjo svetlobnega mikroskopa (OM), spektroskopijo povratno sipanih elektronov na vrstičnem elektronskem mikroskopu (SEM/EBSD) in presevno elektronsko mikroskopijo (TEM). Feritno jeklo so ohlajali s končnih ohlajevalnih temperatur 663 °C in 560 °C in pri tem ustvarili mešano feritno-perlitno mikrostrukturo. Pri znižanju končne temperature ohlajanja na 560 °C se je velikost feritnih kristalnih zrna zmanjšala s 3,15 μm na 2,67 μm. Opazili so, da se je povečal delež igličastega in poligonalnega ferita. Tako so pomaknili pojav začetka krhkega loma jekla celo do –110 °C in s tem močno izboljšali udarno žilavost jekla pri zelo nizkih temperaturah v primerjavi z ostalimi jekli te vrste.

Ključne besede: feritno jeklo; termomehansko kontroliran proces; morfologija feritnih kristalnih zrn, kriogenska udarna žilavost

1 INTRODUCTION

Steels have been widely used in infrastructure, heavy machinery and other fields. In order to reduce the weight and improve the safety of transportation, it is necessary to enhance the cryogenic toughness of steels. However, strength and toughness are usually mutually exclusive in conventional metals.[1–4] Nearly all steels show a ductile-brittle transition. Hence, it is important to develop steels with an excellent cryogenic toughness.

Grain refinement is an effective way to lower the ductile-brittle transition temperature (DBTT) of high-strength steels. However, when the grain size is refined below 1 μm, the plasticity and toughness of the steel are significantly reduced.[5–7] Delamination or splitting caused by anisotropic microstructures (such as the orientation of grains and the second phase along the rolling direction) can improve the toughness of metals at low temperatures. However, in the process of reducing the DBTT, delamination toughening usually reduces the toughness of the ductile fracture zone.[8–9] In addition, Mg-Ni-Ti composite materials with dual, continuous, interpenetrating phase structures can be developed through three-dimensional printing technology. The composite material has a unique combination of mechanical properties, such as good energy-absorption efficiency and better strength and toughness indicators, and its strength can be improved efficiently at ambient temperature and even at high temperature.[10] Some researchers also improved the strength and toughness by developing high-entropy alloys.[11] Nickel can be added to greatly improve the strength of the steel and keep the steel's good toughness.[12] Medium-manganese steel has been widely studied due to its reasonable cost and excellent mechanical properties. In medium-manganese steel, by adjusting the microstructure of the retained austenite, steels with good strength and toughness indexes can be obtained.[13]

*Corresponding author's e-mail:
gaopeng20060707@163.com, (Peng Gao)

Table 1: Chemical composition of the steel (*w*).

C	Si	Mn	Al	Nb	Ti	Cu	Ni	Cr	P	S	N
0.08	0.13	1.52	0.044	0.016	0.012	0.12	0.12	0.015	0.0063	0.0006	0.0034

Table 2: The parameters of thermo-mechanical processing.

Steel	T_{in} of rough rolling, °C	T_{out} of rough rolling, °C	T_{in} of finish rolling, °C	T_{out} of finish rolling, °C	T_{out} of cooling, °C	Cooling time, s	Colling rate, °C/s
LT	1026	995	817	827	560	12	20.58
HT	1032	992	877	852	663	12	14.08

To ensure the low-temperature impact toughness of the steel plate, low-carbon, ultra-low-sulfur and inclusion morphology control are adopted in the steelmaking process. When the content of sulfur and phosphorus in the steel is high, the impact toughness is little affected at high temperature, but the impact toughness is sensitive to sulfur and phosphorus at low temperature. Therefore, it is of great significance to improve the strength and toughness of steel plate by adopting a pure smelting technology and controlling the content of sulfur and phosphorus at the minimum value.[14–16]

In this paper the mechanical properties and microstructure of ferritic steel were researched for the mechanism of improving the strength and toughness of steel plate. Pure smelting technology was used to control the content of sulfur and phosphorus. The effects of the final cooling temperature on the microstructures and mechanical properties were researched. A steel plate with excellent comprehensive mechanical properties was obtained by multi-type and fine-microstructure design.

2 EXPERIMENTAL PART

2.1 Materials

To fabricate high-quality ferritic steel with high strength and cryogenic toughness, a series of processes including a hot metal pre-treatment, converter blowing and RH vacuum refining were adopted to reduce the contents of phosphorus, sulfur and nitrogen in the steel. It is important to control a reasonable chemical composition to improve the strength and toughness of steel.[17,18] The chemical composition of the steel is shown in **Table 1**.

2.2 Thermo-mechanical processing

The rolling experiment was carried out on a 450-mm rolling mill. The conventional two-stage rolling was adopted. According to the empirical formula of T_{NR},[19] the estimated non-recrystallization temperature of the steel is 924 °C. Therefore, the final rolling temperature of recrystallization-controlled rolling is in the temperature range 1000–1020 °C and the initial rolling temperature of recrystallization-controlled rolling is controlled at 1050 °C. The final temperature of non-recrystallization-controlled rolling is about 850 °C. In addition, according to the empirical formula of A_{e3},[20] the estimated A_{e3} temperature of the steel is 786 °C, which is like the thermodynamic calculation result of 820 °C. According to the empirical formula of A_{e1}, the estimated A_{e1} temperature of the steel is 709 °C. Considering that the A_{r1} temperature is lower than the A_{e1} temperature, the final set cooling temperature of 550 °C and 650 °C was chosen. The schematic diagram of thermo-mechanical control process is shown in **Figure 1**, and the actual measured parameters of thermo-mechanical control process are shown in

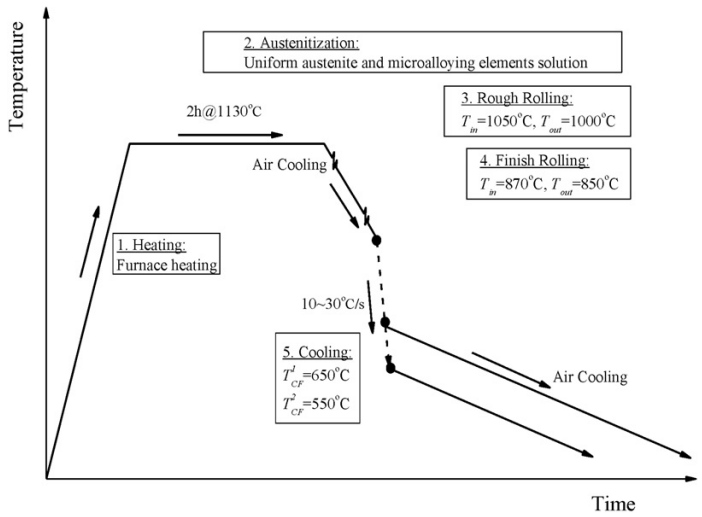

Figure 1: Schematic diagram of thermo-mechanical processing

Table 2. Moreover, the steel with a low final actual measured cooling temperature of 560 °C is designated as "low-temperature (LT) steel", while the one with a high final actual measured cooling temperature of 663 °C is designated as "high-temperature (HT) steel".

2.3 Microstructure characterization and mechanical property tests

The samples for microstructure characterization were cut from the hot-rolled plates, and the longitudinal section was polished and etched in 4 % nitric alcohol solution for ≈15 s. The microstructure was observed on an optical microscope (LEICA DMIRM). In addition, the metallographic samples were used for EBSD analysis after electropolishing. The electrolyte contained 12.5 % perchloric acid and 87.5 % absolute ethanol. The voltage, current and time of electropolishing were 30 V, 1.8 A and 15 s, respectively.

A CMT-5105 tensile testing machine was used to measure the strength and ductility along the rolling direction. Three specimens were tested for each batch. The tensile samples were machined and stretched according to GB/T 228-2002. The Charpy V-notch impact samples of 10 mm × 10 mm × 55 mm was tested with a JBW-500 impact testing machine at different temperatures, and the test is in accordance with GB / T 229-1994 national standard. The testing temperatures were 20 °C, –40 °C, –80 °C and –110 °C. The samples for TEM analysis were cut from the hot-rolled plate with a wire-cutting machine. The thickness was reduced to less than 45 μm with abrasive paper, and then some wafers with a diameter of 3 mm were punched using a Dervee 1700-3A puncher. Then these wafers were further thinned with a twin-jet electrolytic polisher in 10 % perchloric acid alcohol solution, and the operating voltage and temperature were 32 V, –20 °C, respectively. Finally, these samples were examined in a Fei TECNAI G² F20 transmission electron microscope (TEM) operated at 200 kV.

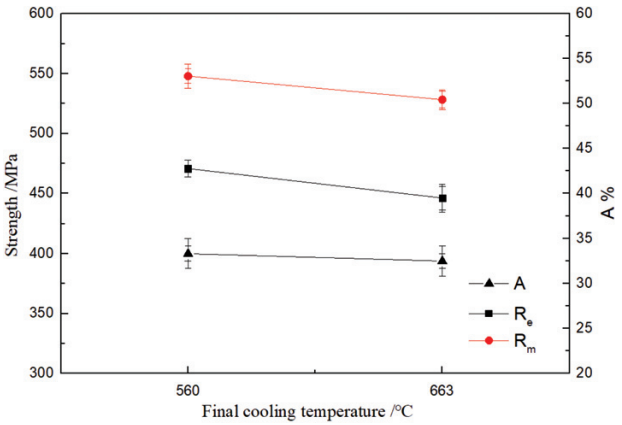

Figure 2: Tensile properties of the LT and HT steels

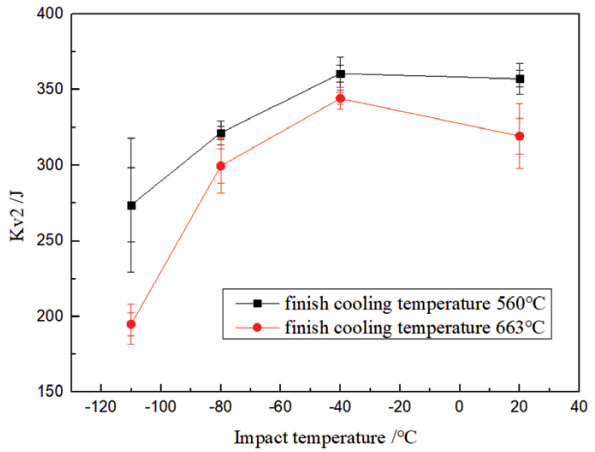

Figure 3: Impact absorbed energy of the LT and HT steels at different temperature

3 RESULTS

3.1 Mechanical properties

The yield strength, tensile strength and total elongation of the steels are shown in **Figure 2**. Both the yield strength and tensile strength can be slightly enhanced by lowering the final cooling temperature. Both steels show similar ductility. The impact absorbed energy of the steels is shown in **Figure 3**, revealing that the impact absorbed energy of the LT steel is higher than that of the HT steel, especially at –100 °C.

3.2 Optical microstructure

The microstructures of the LT and HT steels are shown in **Figure 4**. Both steels show ferrite and pearlite

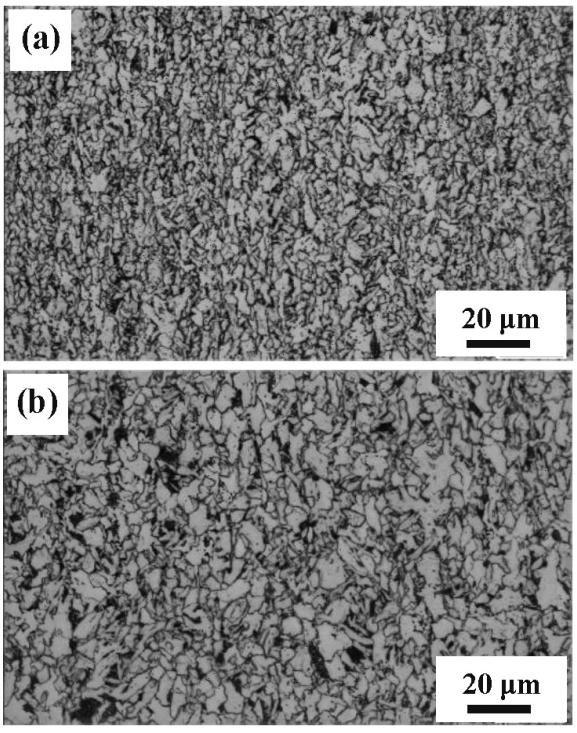

Figure 4: Microstructure of: a) LT and b) HT steels

Table 3: Grain size of the LT and HT steels.

steel	<1μm	<3μm	<5μm	<7μm	<9μm	<11μm	<13μm	<15μm	<17μm	<23μm	<29μm	<33μm	<39μm
LT	63.062	25.181	7.257	1.887	1.306	0.508	0.435	0.0726	0.145	0.0726	0.0726	0	0
HT	60.423	20.282	9.296	4.085	1.972	0.845	0.845	0.563	0.704	0.563	0.141	0.141	0.141

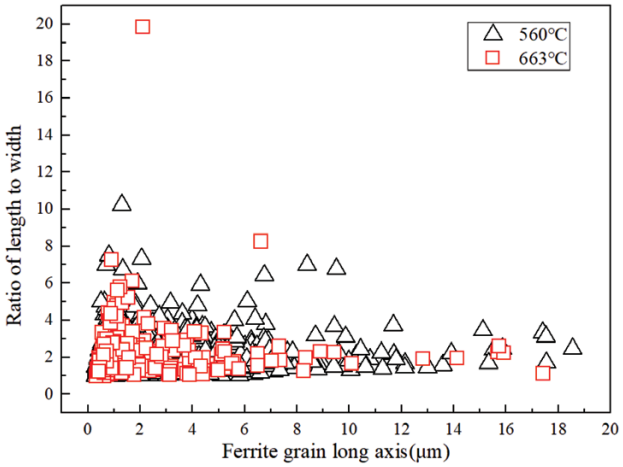

Figure 5: Grain morphology of the LT and HT steels

microstructures. Among them, ferrite accounted for a large proportion (82–93 %). The grain size of the LT steel is relatively small and the grain boundary was serrated. The grain size of the HT steel was large and the grain boundary was smooth. The comparison of the grain sizes is shown in **Table 3**. The average grain size of the LT steel was smaller than that of the HT steel, and the number fraction of grains with a size below 5 μm is also high in the LT steel. This is because the undercooling at the final cooling temperature of 560 °C is larger than that at the final cooling temperature of 663 °C, which gives full play to the role of ultra-fast cooling in the phase transformation region and is beneficial to the grain refinement. **Figure 5** shows the distribution of the grains' long axes with different final cooling temperatures. The long axis of most grains was below 10 μm and the aspect ratio was below 6.

3.3 EBSD analysis

The EBSD results are shown in **Figure** 6. The grain size distribution of both processes is shown in **Figure 7**.

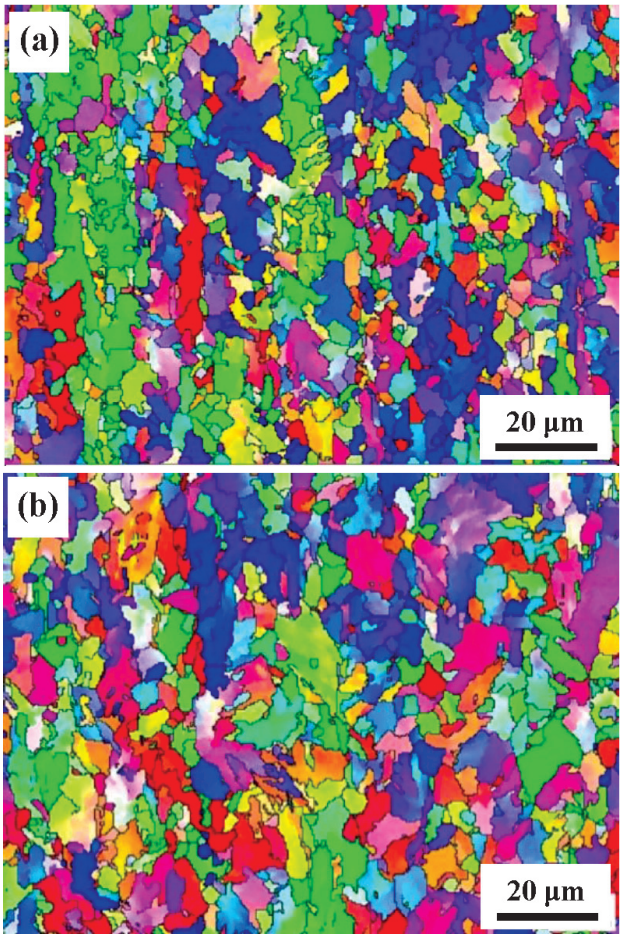

Figure 6: EBSD analysis on: a) LT and b) HT steels

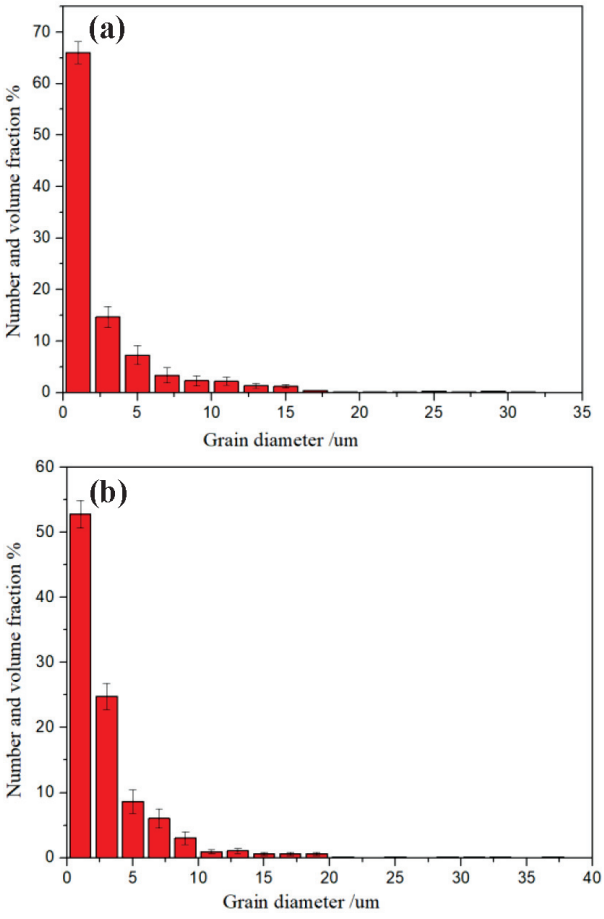

Figure 7: Grain size distribution of: a) LT and b) HT steels

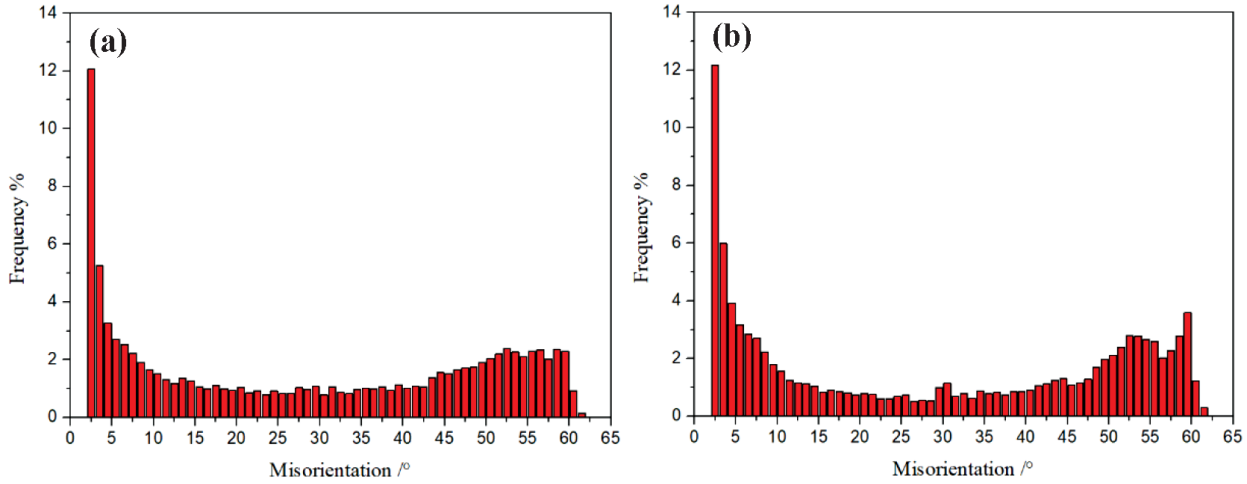

Figure 8: Misorientation distribution of the a) LT and b) HT steels

The average grain size in **Figure 7a** was 2.67 μm, and that in **Figure 7b** was 3.15 μm. The grain misorientation statistics are shown in **Figure 8**. The number fraction of high-angle grain boundaries in **Figure 8a** was 61.8 %, and that in **Figure 8b** was 59.15 %. At a low final cooling temperature of 560 °C, the grain size was small, and the proportion of high-angle grain boundaries was high, resulting in better overall mechanical properties.

It is concluded that the final cooling temperature of 560 °C can lead to a fine microstructure, high yield strength, tensile strength and impact energy. This is because the grain size mainly depends on the nucleation rate and growth rate. With the increase in undercooling, the nucleation rate and growth rate increase, but the increasing rate is different. When the undercooling is small, the increasing rate of the nucleation rate is less than the growth rate. However, when the undercooling is large, the increasing rate of nucleation rate is greater than the growth rate. During the transformation of austenite to ferrite, the grain size of ferrite and pearlite can be refined by increasing the undercooling. The higher the cooling rate is, the greater the undercooling is. Therefore, an increasing cooling rate is conducive to refining the grain size and improving the strength and toughness.

3.4 TEM analysis

Figure 10 shows the TEM microstructure and precipitate morphology of the LT and HT steels. The microstructure with a final cooling temperature of 560 °C was composed of acicular ferrite and polygonal ferrite. The ferrite grain was fine. The diameter of smallest polygonal ferrite grain was about 200 nm, and the width of acicular ferrite was about 220 nm. Dislocations begin to

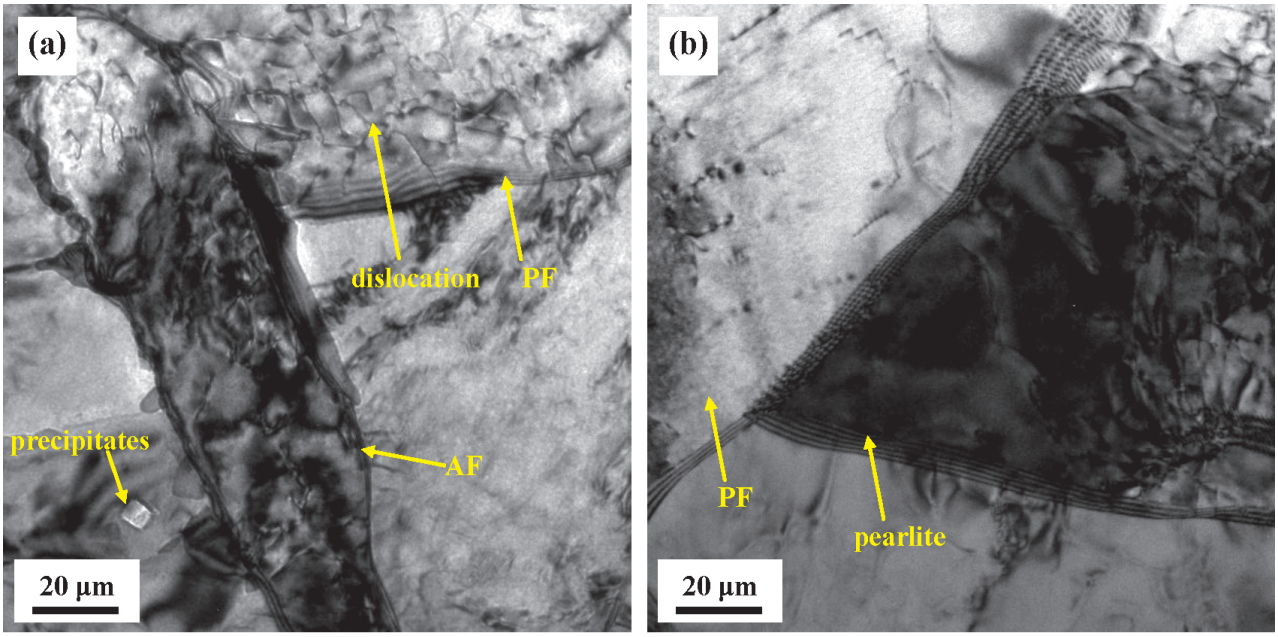

Figure 9: TEM micrographs of the a) LT and b) HT steels

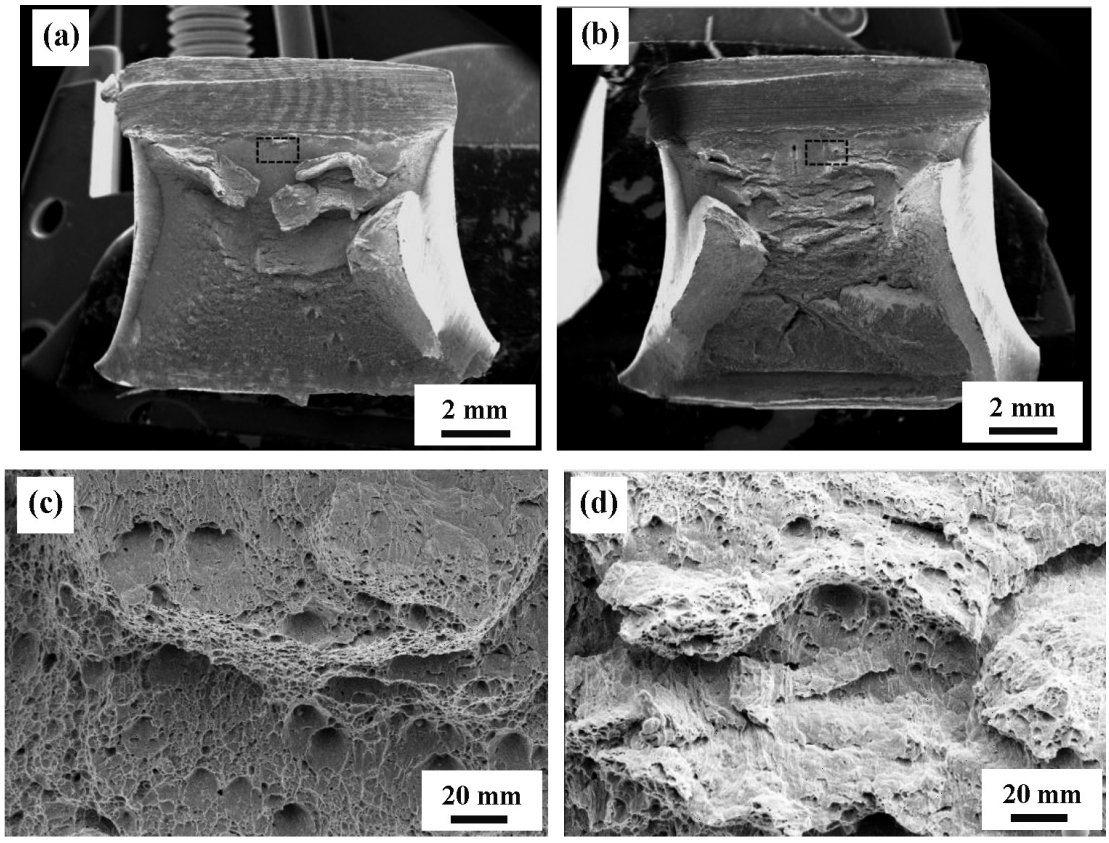

Figure 10: Impact fractographs of the LT steel: a), c) –40 °C, b), d) –110°C

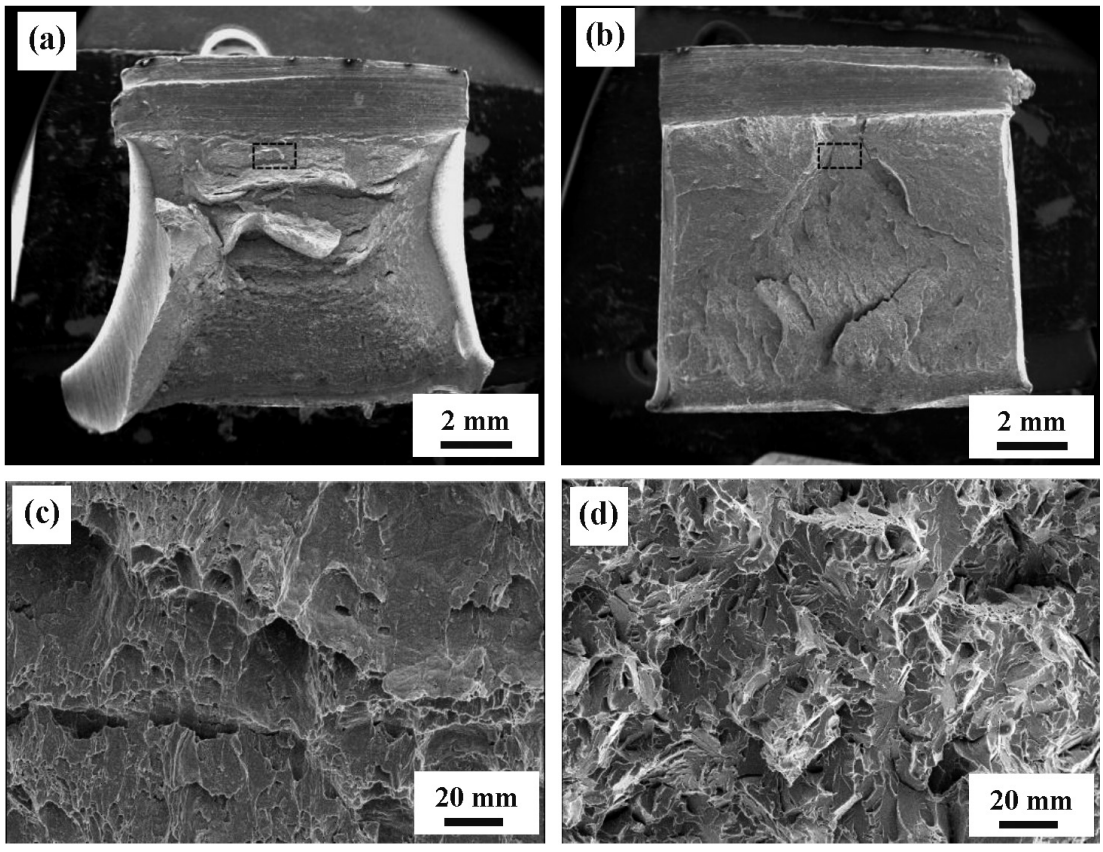

Figure 11: Impact fractographs of the HT steel: a), c) –40 °C, b), d) –110°C

migrate within the polygonal ferrite and at the grain boundaries. There were carbide precipitates in the polygonal ferrite with the size about 50 nm. The microstructure with the final cooling temperature of 663 °C was mainly composed of polygonal ferrite and pearlite. The polygonal ferrite had larger grain size, fewer dislocations and no carbide precipitation.

3.5 Impact fractographs

Figure 10 shows the impact fractographs of the LT steel. The shear lip and fiber zone of the fracture surface at –40 °C and –110 °C were large, and the radiation zone was small, resulting in a higher impact energy. As shown in **Figure 10c**, many ovate dimples with certain directions were seen, which were deep and flat at the bottom. Some small dimples were also distributed in coarse dimples. The directivity of the dimples indicates that the sample is fractured by tearing, and the tearing needs to absorb a lot of energy. As shown in **Figure 10d**, coarse dimples and a certain number of small dimples were seen. However, there were some river patterns. The fracture surface was composed of fiber zone and cleavage zone, but mainly in the fiber zone. Therefore, the sample still maintains a high toughness.

Figure 11 shows the impact fractographs of the HT steel. At –40 °C, the shear lip and fiber zone were larger than the radiation zone, resulting in a higher impact energy. The fracture surface at –110 °C is a typical brittle fracture mode with low impact energy. As shown in **Figure 11c**, there was mainly the fiber zone, and many ovate dimples were seen. The dimples were deep, and thus the toughness is better. As shown in **Figure 11d**, there were fewer small dimples and many river patterns. The fracture surface was mainly composed of cleavage zone.

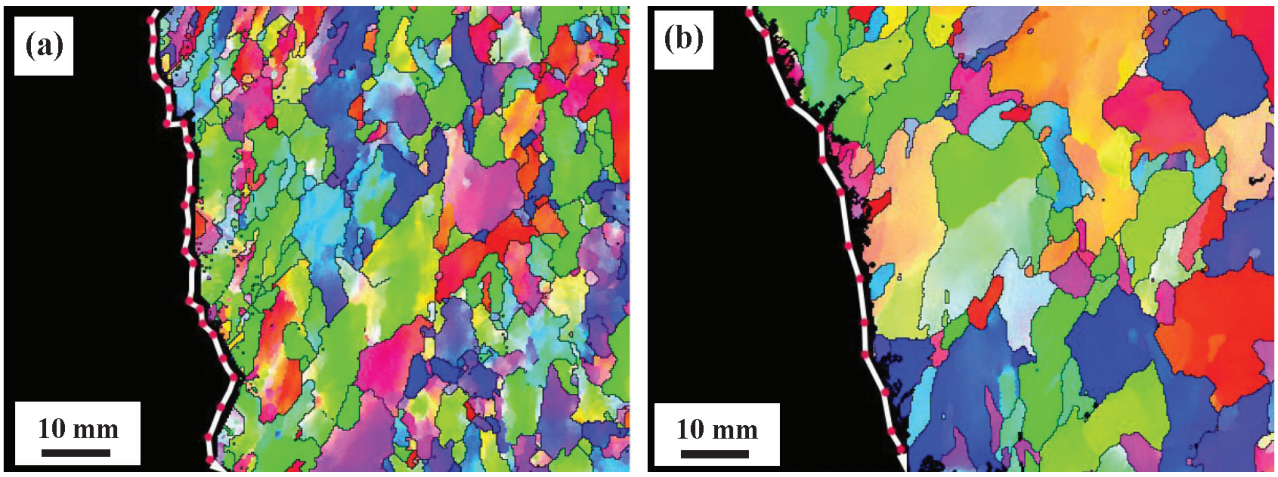

Figure 12: EBSD micrographs of the a) LT and b) HT steels

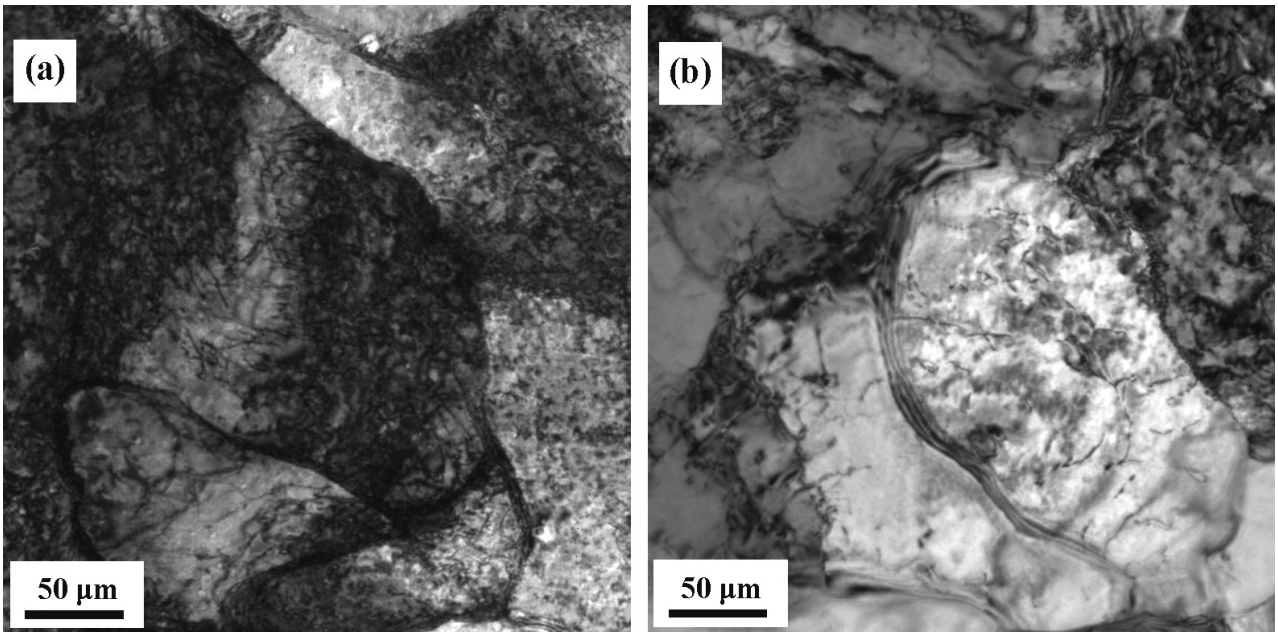

Figure 13: TEM micrographs beneath fracture surface of: a) LT and b) HT steels

Therefore, the toughness is relatively low and the impact absorbed energy is 190 J.

4 DISCUSSION

4.1 Crack propagation

The microstructure beneath the fracture surface was characterized by EBSD, as shown in **Figure 12**. The crack prolongation paths were depicted by white lines in **Figure 12a** and **12b**, with the decrease of final cooling temperature, the more tortuous crack propagation path can be observed. The finer grain size caused by a lower final cooling temperature of 560°C resulted in a higher volume fraction of high-angle grain boundaries (HAGBs). Many researchers indicated that the ferrite with HAGBs can effectively prevent crack propagation.[19–20] Thus, the impact toughness is obviously enhanced.

The substructure near by the main crack after the impact test at –110 °C was characterized by TEM, as shown in **Figure 13**. Polygonal ferrite grain of 600 nm and acicular ferrite of 220 nm with high density dislocation caused by a lower final cooling temperature of 560 °C are observed. It is obviously that grain boundaries can prevent the slip of dislocations. So that dislocations are more likely to become entangled at grain boundaries due to the higher volume fraction of HAGBs (**Figure 8a**), which contributed to a higher impact toughness. However coarse grain with lower volume fraction of HAGBs under a higher final cooling temperature of 663 °C exhibited a lower impact toughness.

5 CONCLUSIONS

Steels with two different final cooling temperatures were obtained by combinations of pure smelting and controlled rolling and ultra-fast cooling. The microstructure and mechanical properties of the steels were investigated.

(1) The microstructure of both steels is composed of ferrite and pearlite. However, a lower final cooling temperature of 560 °C can refine the ferrite grains and the average grain size is refined from 3.15 μm to 2.67 μm by lowering the final cooling temperature from 663 °C to 560 °C. The grain-refinement effect is not pronounced. This may be a main reason why the tensile strength is not greatly enhanced.

(2) Note that a lower final cooling temperature of 560 °C can greatly change the ferrite grain morphology, resulting a higher volume fraction of acicular ferrite and polygonal ferrite. Hence, the cryogenic impact toughness can be enhanced, and the brittle failure can be suppressed even at –110 °C.

Author contribution statement

Z.-Y. L. and Z.-C. L. conceived the experiments; P. G. and C.-G. Li performed the experiments; Z.-C. L. and P. G. wrote the paper; W.-B. Zhong and Z. H. processed the data; J.-K. R. revised the paper and contributed to the discussion of the results.

Declaration of competing interest

The authors declare that they have no known competing financial interests or personal relationships that could have appeared to influence the work reported in this paper.

Acknowledgments

This work was supported by the Dedicated Fund for Promoting High-Quality Economic Development in Guangdong Province (Marine Economic Development Project) (grant number GDOE[2019]A08), and also was supported by Science and Technology Research Project of Jiangxi Provincial Department of Education (grant number GJJ211821).

Data availability

The raw/processed data required to reproduce these findings cannot be shared at this time as the data also forms part of another ongoing study.

6 REFERENCES

[1] Y. Kimura, T. Inoue, F. Yin, K. Tsuzaki, Inverse temperature dependence of toughness in an ultrafine grain-structure steel, Science, 320 (**2008**), 1057–1060, doi:10.1126/science.1156084

[2] L. Liu, Qin Yu, Z. Wang, J. Ell, M. Huang, R. Ritchie, Making ultrastrong steel tough by grain-boundary delamination, Science, 368 (**2020**), 1347–1352, doi:10.1126/science.aba9413

[3] K. Lu, The future of metals, Science, 328 (**2010**), 319–320, doi:10.1126/science.1185866

[4] J. Reiser, A. Hartmaier, Elucidating the dual role of grain boundaries as dislocation sources and obstacles and its impact on toughness and brittle-to-ductile transition, Sci. Rep, 10 (**2020**), 1–18, doi:10.1038/s41598-020-59405-5

[5] J. Wu, B. Wang, B. Wang, R. Misrab, Z. Wang, Toughness and ductility improvement of heavy EH47 plate with grain refinement through inter-pass cooling, Mater. Sci. Eng. A, 733 (**2018**), 117–127, doi:10.1016/j.msea.2018.07.001

[6] R. Song, D. Ponge, D. Raabe, Mechanical properties of an ultrafine grained C-Mn steel processed by warm deformation and annealing, Acta Mater, 53 (**2005**), 4881–4892, doi:10.1016/j.actamat.2005.07.009

[7] A. Karimpoor, K.Aust, U. Erb, Charpy impact energy of nanocrystalline and polycrystalline cobalt, Scripta Mater, 56 (**2007**), 201–204, doi:10.1016/j.scriptamat.2006.10.018

[8] B. Mintz, A. Williamson, H. Su, W. B. Morrison, Influence of nitride formers on strength and impact behavior of hot rotted steel, Mate Sci and Technol, 23 (**2007**), 63–71, doi:10.1179/174328407X158415

[9] J. W. Morris Jr, Stronger tougher steels, Science, 320 (**2008**), 1022–1023, doi:10.1126/science.1158994

[10] M. Zhang, Q. Yu, Z. Liu, J. Zhang, RO. Ritchie, 3D printed Mg-NiTi interpenetrating-phase composites with high strength, damping capacity, and energy absorption efficiency, Sci Adv, 6 (**2020**), 1–9, doi:10.1126/sciadv.aba5581

[11] B. Gludovatz, A. Hohenwarter, D. Catoor, E. Chang, E. George, RO. Ritchie, A fracture-resistant high-entropy alloy for cryogenic applications, Science, 345 (**2014**), 1153–1158, doi:10.1126/science.1254581

[12] H. Kong, C. Xu, C. Bu, C. Da, J. Luan, Z. Jiao, G. Chen, C. Liu, Hardening mechanisms and impact toughening of a high-strength steel containing low Ni and Cu additions, Acta Mater, 172 (**2019**), 150–160, doi:10.1016/j.actamat.2019.04.041

[13] M. Jeong, T. Park, S. Choi, S. Lee, J. Han, Recovering the ductility of medium-Mn steel by restoring the original microstructure, Scr Mater, 190 (**2021**), 16–21, doi:10.1016/j.scriptamat.2020.08.022

[14] H. Tervoa, A. Kaijalainena, T. Pikkarainen, S. Mehtonen, D. Porter, Effect of impurity level and inclusions on the ductility and toughness of an ultra-high-strength steel, Mate. Sci. Eng. A, 697 (**2017**), 184–193, doi:10.1016/j.msea.2017.05.013

[15] W. Bielefeldt, A. Vilela, Study of inclusions in high sulfur, al-killed ca-treated steel via experiments and thermodynamic calculations, Steel Res Int, 86 (**2015**), 375–385, doi:10.1002/srin.201400112

[16] A. Gupta, S. Goyal, K. Padmanabhan, A. Singh, Inclusions in steel: micro–macro modelling approach to analyse the effects of inclusions on the properties of steel, Int. J. Adv. Manuf. Tech, 77 (**2015**), 565–572, doi:10.1007/s00170-014-6464-5

[17] A. Zaitsev, A. Koldaev, N. Arutyunyan, S. Dunaev, D. D'yakonov, Effect of the chemical composition on the structural state and mechanical properties of complex microalloyed steels of the ferritic class, Processes, 8 (**2020**), 646–657, doi:10.3390/pr8060646

[18] C. Wang, M. Wang, J. Shi, W. Hui, H. Dong, Effect of microstructural refinement on the toughness of low carbon martensitic steel, Scr. Mater, 58 (**2008**), 492–495, doi:10.1016/j.scriptamat.2007.10.053

[19] K. Andrews. Empirical formulae for calculation of some transformation temperatures, J I S I, 203 (**1965**), 721–727

[20] B. Hwang, C. Lee, S. Kim, Low-temperature toughening mechanism in thermo-mechanically processed high-strength low-alloy steels, Metal Mater Trans A, 42 (**2011**), 717–728, doi:10.1007/s11661-010-0448-3